ELSEVIER

Chemical Engineering Journal 131 (2007) 105–111

Chemical Engineering Journal

www.elsevier.com/locate/cej

Gas holdup and mixing characteristics of a novel forced circulation loop reactor

Ali Fadavi [a,*], Yusuf Chisti [b]

[a] *Department of Farm Machinery, Faculty of Agricultural Engineering, Ilam University, Ilam, Iran*
[b] *Institute of Technology and Engineering, Massey University, Private Bag 11 222, Palmerston North, New Zealand*

Received 15 May 2006; received in revised form 14 December 2006; accepted 18 December 2006

Abstract

Gas holdup and mixing time were characterized in a forced circulation internal loop draft-tube reactor (unaerated aspect ratio ≈ 6, downcomer-to-riser cross-sectional area ratio = 0.493) as functions of the forced liquid superficial velocity in the riser (U_{Lr}) and the gas superficial velocity in the riser (U_{Gr}). Data were obtained in air–water system. The operation ranges were $0 \leq U_{Lr} \leq 0.051$ m/s and $7.8 \times 10^{-3} \leq U_{Gr} \leq 3.9 \times 10^{-2}$ m/s for the liquid and gas velocities, respectively. Under forced flow conditions the reactor always operated in the bubble flow regimen, but operation as an airlift reactor (i.e. no forced flow of liquid) produced a heterogeneous churn-turbulent flow regimen. Forced flow of liquid enhanced gas holdup in comparison with the airlift mode of operation. Mixing time generally declined with increased flow rates of gas and liquid. The ability to maintain a bubble flow regimen through forced flow of liquid allowed the reactor to attain gas holdup values of >0.12 that are difficult to achieve in air–water in conventional bubble columns and airlift reactors.

Keywords: Gas holdup; Mixing time; Power consumption; Forced circulation loop reactor; Jet loop reactor; Airlift bioreactor

1. Introduction

Gas–liquid reactors are commonly used in industrial processes that involve absorption or desorption of a gas. Examples of such reactors include bioreactors that are used in aerobic microbial and cell culture processes. Two frequently used types of gas–liquid reactors are the bubble column and airlift loop reactor in which mixing is achieved solely through the action of the injected gas. Effective use of these reactors generally requires a homogenous bubble flow regimen of operation that is characterized by the presence of ellipsoidal bubbles of a relatively uniform size (typically ≤0.9 m in major diameter in air–water systems). Uniformly sized small bubbles have a relatively high specific interfacial area for gas–liquid mass transfer compared with larger spheroidal or spherical cap bubbles. The latter coexist with small bubbles once the flow regime changes to churn-turbulent or heterogeneous flow.

Flow regimen transition from bubble flow to churn-turbulent flow occurs at relatively low values of gas injection rates in bubble columns and airlift reactors. This flow transition has associated adverse outcomes, including poor contact of the gas and liquid phases, a broad residence time distribution of the gas phase and reduced efficiency in gas–liquid mass transfer. Reactor designs that can extend the bubble flow regimen of operation to higher values of gas flow rates than in bubble columns and airlift reactors, are potentially useful [1].

This work reports on characterization of gas holdup and liquid phase mixing in a forced circulation loop reactor with a novel type of gas sparger, for possible use as a gas–liquid contactor. The use of a novel sparger design in combination with forced circulation of the liquid through an external centrifugal pump, is shown to substantially extend the range of gas flow rates at which the desirable bubbly flow regime can be maintained in the reactor. Other designs of forced circulation loop reactors have been reported in the literature [2–4], but they did not use gas spargers that were specifically designed to control bubble size. Single orifice nozzles were generally used in the past for injecting the gas and this often lead to a heterogeneous flow regimen.

* Corresponding author at: Department of Farm Machinery, Faculty of Agricultural Engineering, Ilam University, P.O. Box 69315-516, Ilam, Iran. Tel.: +98 841 2228059; fax: +98 841 2227015.
E-mail address: a_fadavi@yahoo.com (A. Fadavi).

1385-8947/$ – see front matter © 2007 Elsevier B.V. All rights reserved.
doi:10.1016/j.cej.2006.12.037

Nomenclature

e_T	power input per unit volume (W/m^3)
g	gravitational acceleration (m/s^2)
ΔH	vertical distance between the pressures taps (m)
H_L	unaerated liquid height (m)
L_M	mixing tube length (m)
M	molar mass (kg/kmol)
ΔP_R	differential pressure between pressure taps in riser or downcomer (Pa)
ΔP_s	differential pressure between inlet and outlet of sparger (Pa)
P_t	pressure at top section (Pa)
Q_L	volumetric liquid flow rate (l/h)
Q_m	molar gas flow rate (kmol/s)
R	universal gas constant (J/kmol K)
T	temperature (K)
U_G	superficial gas velocity in bubble column (m/s)
U_{Gr}	superficial gas velocity in riser (m/s)
U_{Lr}	superficial liquid velocity in riser due to forced circulation (m/s)
v_{LN}	liquid velocity in nozzle (m/s)
v_o	gas velocity through the sparger hole (m/s)
V_L	liquid volume in the reactor (m^3)

Greek symbols

ε	gas holdup
ρ	density (kg/m^3)
Ω	efficiency factor

Subscripts

d	downcomer
D	dispersion
G, g	gas phase
L	liquid phase
r	riser
T	total

2. Materials and methods

2.1. Internal-loop reactor

Measurements were made in a novel design of an internal loop recirculation reactor (Fig. 1). The reactor consisted of a gas–liquid sparger zone (Fig. 1) connected to cylindrical vessel that had a concentric draft-tube downcomer zone. The gas–liquid sparger (Fig. 1) had separate inlets for gas and liquid. Just before the liquid entered the gas injection zone, it passed through a static mixer that produced a spinning or swirling motion of the liquid [5]. The gas was injected into swirling liquid though holes located at the periphery of the conical region of the sparger, as illustrated in Fig. 1. The swirling motion of the liquid past the gas injection point caused the bubbles to be detach and sweep away from the injection holes while they were still relatively small. The exact size of the bubbles at detachment depended on the rates of gas and liquid flow. Smaller bubbles were produced at relatively low values of gas flow rate in combination with high values of liquid flow rate. Air and water were used at the liquid and gas phases, respectively.

Table 1
Reactor geometry and operational parameters

Description	Value
Bioreactor diameter (m)	0.1484
Unaerated liquid height (m)	0.914
Liquid height above draft-tube (m)	0.032
Working volume (m^3)	0.01625
Downcomer-to-riser cross section area ratio (–)	0.493
Draft-tube length (m)	0.865
Inner diameter of draft-tube (m)	0.083
Static mixer	20 mm length, 45° inclination angle
Mixing tube length L_M (m)[a]	0.124, 0.236

[a] Data were obtained with the shorter tube, except for Fig. 8.

Geometric details of the reactor are shown in Table 1. The reactor was piped to the liquid circulation pump, as shown in Fig. 2. A heat exchanger placed in the circulation piping was used to control temperature. Air was supplied from a compressor through a pressure regulator, control valve, rotameter and buffer tank to facilitate precise control of flow rate. A differential pressure transmitter (Rosemount 3051, USA) was used to measure the pressure difference between the inlet and outlet of the sparger zone. The pressure measurement points are shown in Fig. 2. At any steady state, the differential pressure was sampled at 1 s intervals for 30 s and data were recorded using a computer. All experiments were carried out with air and water at 20.5 ± 1.0 °C.

2.2. Measurements

Overall gas holdup was measured using the volume expansion method [6]. Gas holdup values in the riser and downcomer zones were calculated from the differential pressure measurements in these zones, as follows:

$$\varepsilon = \frac{\Delta P_R}{(\rho_L - \rho_G)g\Delta H} \quad (1)$$

where ΔP_R is the pressure differential between measurement points in the riser or downcomer, ρ_L and ρ_G are densities of the gas and liquid phases, respectively, g is gravitational acceleration and ΔH is the vertical distance between the pressure taps in the relevant measurement zone. At every hydrodynamic steady state, 30 measurements of ΔP_R were used to calculate the average holdup.

The power delivered to the reactor was derived from the gas and liquid phases. The total specific energy input e_T was calculated [6–8] as follows:

$$e_T = \frac{Q_m RT}{V_L}\ln\left(1 + \frac{\rho_L g H_L}{P_t}\right) + \frac{\Omega}{2V_L}Q_m M v_o^2 + \frac{Q_L}{2V_L}\rho_L v_{LN}^2 + \frac{\Delta P_s Q_L}{V_L} \quad (2)$$

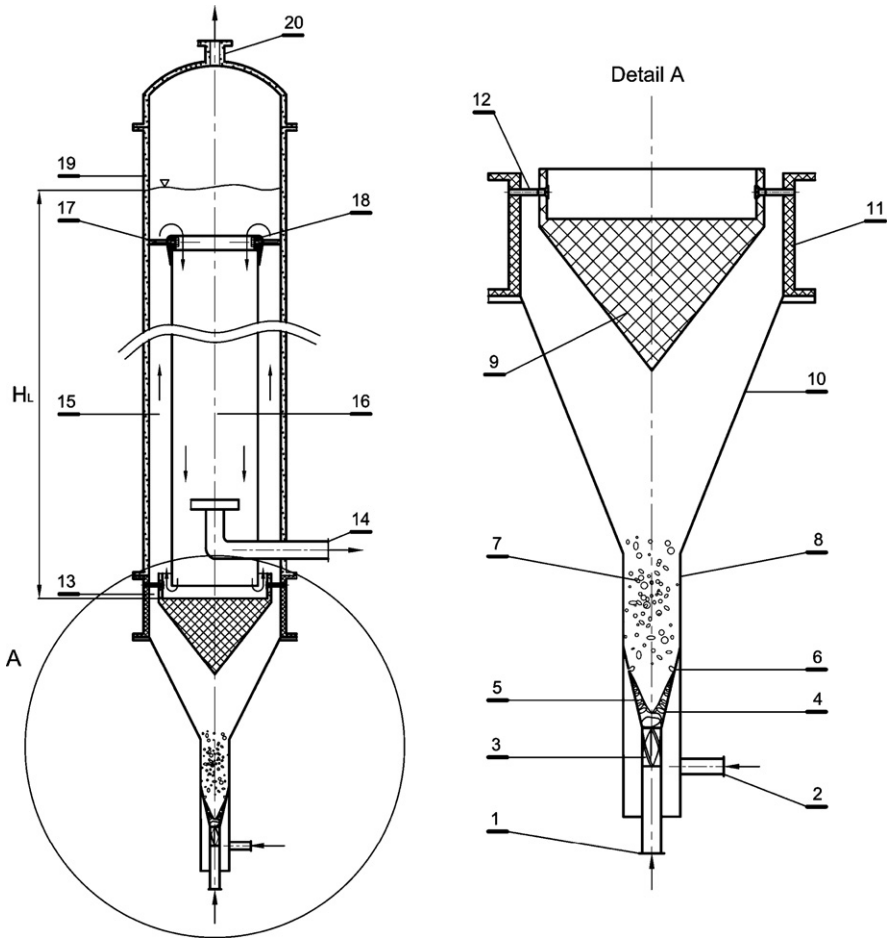

Fig. 1. Details of the reactor: (1) liquid inlet; (2) gas inlet; (3) static mixer; (4) gas sparger; (5) conical liquid input zone; (6) orifice; (7) two-phase mixture; (8) mixing tube; (9) guiding cone; (10) diffuser; (11) support; (12) screw; (13) riser venturi entrance; (14) liquid outlet; (15) riser; (16) downcomer; (17) screw; (18) draft-tube support; (19) reactor vessel; (20) gas outlet.

The first, second, third and fourth terms on the right-hand-side of Eq. (2) represented power input due to isothermal expansion of the gas, the kinetic energy of the injected gas, the kinetic energy of the liquid entering the reactor, and the energy loss in the sparger zone. The efficiency factor Ω was taken to be 1 [6]. Derivation of the first two terms of Eq. (2) has been discussed in detail previously [6]. Terms three and four in the above equation have been commonly derived in textbooks dealing with fluid flow in pipes [9].

Mixing time was measured by the conductivity method [10] using saturated sodium chloride solution as the tracer. For each measurement, 60 ml of the tracer solution was rapidly injected into the mixing tube (Fig. 2). Conductivity was measured online at 0.02 s intervals using the probes located as in Fig. 2. Mixing time data reported are for the completely mixed state (2% deviation from the equilibrium tracer concentration) from the instance of tracer injection.

3. Result and discussion

3.1. Power input

The total specific power input in the forced circulation reactor increased with increasing flow rates of gas and liquid (Fig. 3); however, in comparison with the liquid flow rate, the gas flow rate had a much lower effect on the total power input. For example, at a constant superficial liquid velocity of 1.3×10^{-2} m/s, a four-fold increase in aeration rate increased the total power input approximately by only four-fold (Fig. 3). In comparison with this, at a constant superficial aeration velocity of 1×10^{-2} m/s, a 4-fold increase in the liquid flow rate increased the total power specific power input by nearly 15-fold (Fig. 3).

3.2. Gas holdup

At any constant value of the liquid injection rate, the overall gas holdup increased with increasing value of the total specific power input, as shown in Fig. 4. The slope of the gas holdup versus specific power input plot for reactor operation in the airlift mode (i.e. $U_{Lr} = 0$ m/s, Fig. 4), was significantly less in comparison with slopes of the plots for operation in the forced circulation mode ($U_{Lr} > 0$ m/s, Fig. 4). Clearly, during operation in the forced circulation mode, the overall gas holdup in the reactor was more sensitive to power input than during operation in the airlift mode.

For nearly all values of the aeration rates during operation as an airlift reactor, a heterogeneous churn-turbulent flow regime

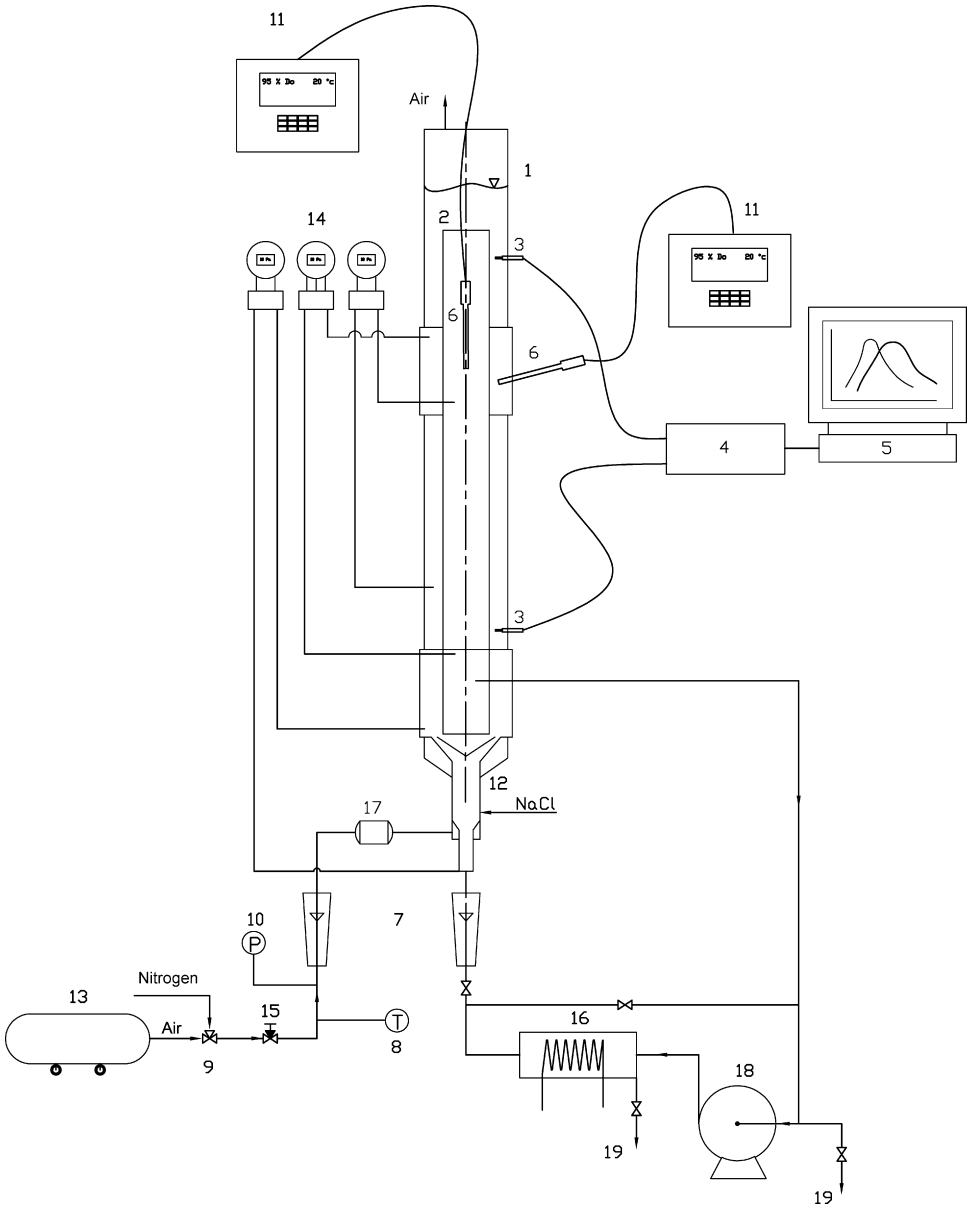

Fig. 2. Schematic of the loop reactor and ancillary equipment: (1) reactor body; (2) draft-tube; (3) conductivity probe; (4) A/D converter; (5) computer; (6) oxygen probe; (7) rotameter; (8) thermometer; (9) three-way valve; (10) pressure gauge; (11) oxygen meter; (12) gas–liquid sparger; (13) compressor; (14) pressure transmitter; (15) needle valve; (16) heat exchanger; (17) buffer tank; (18) centrifugal pump; (19) drain valve.

was observed in the reactor. In contrast, throughout the range of gas and liquid flow rates examined in the forced circulation mode of operation ($U_{Lr} > 0$ m/s), the flow regimen was in bubbly flow (Fig. 5) and no spherical cap gas bubbles existed. This is unlike the case in bubble columns and airlift bioreactors where spherical cap bubble are commonly observed at lower values of gas flow rates than used in this work. Turbulence generated by forced circulation reduced bubble size and prevented heterogeneous flow from occurring at the maximum aeration velocity of 3.9×10^{-2} m/s. Consequently, up to a liquid velocity of 2.5×10^{-2} m/s, generally higher values of the overall gas holdup were achieved in the forced circulation mode than in the airlift mode ($U_{Lr} = 0$ m/s) for identical ranges of the total specific power input (Fig. 4). For any given plot in Fig. 4, any change in the total specific power input was exclusively because of changes in aeration rate. As a consequence of early transition to heterogeneous flow, bubble columns and airlift reactors do not generally exceed an overall gas holdup value of 0.1 in air–water system [6,11]. This was indeed the case for airlift mode of operation in Fig. 4 where the maximum gas holdup was less than 0.08. In contrast, the forced circulation operation at a relatively low liquid velocity of 2.5×10^{-2} m/s attained an overall gas holdup of >0.1 (Fig. 4). Bubble flow regime persisted to a gas holdup value of nearly 0.13 (Fig. 4) during forced circulation operation.

In a loop reactor such as the one used in this work, the overall gas holdup is contributed by the gas holdup in the riser and downcomer zones. The dependence of the riser gas holdup on gas and liquid velocities is shown in Fig. 6. The riser gas holdup was only marginally increased at the lowest liquid veloc-

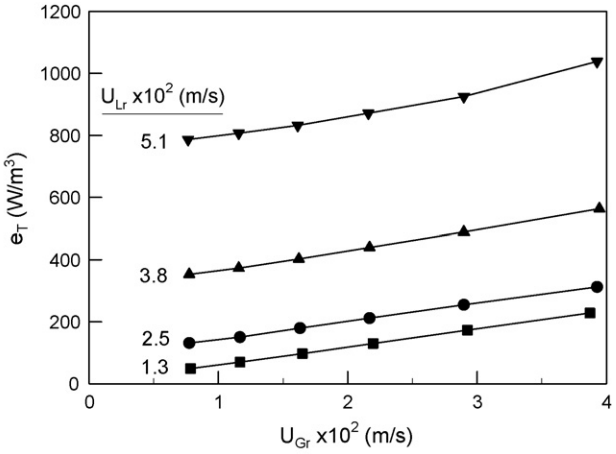

Fig. 3. Total energy (e_T) consumption vs. gas velocity (U_{Gr}) for different values of liquid velocity (U_{Lr}).

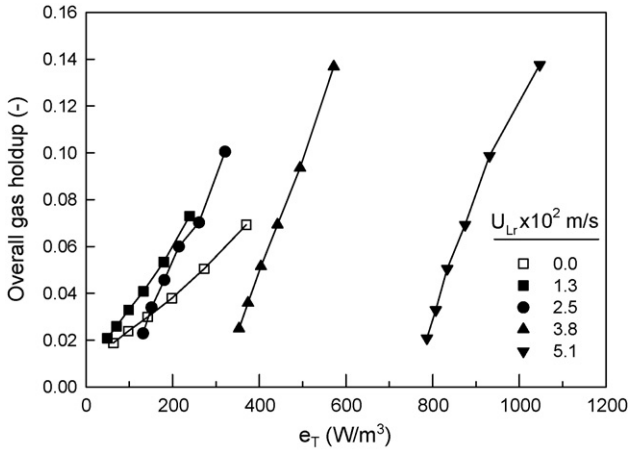

Fig. 4. Influence of total specific energy input (e_T) and forced circulation liquid velocity (U_{Lr}) on overall gas holdup.

Fig. 5. Bubble flow regimen in the reactor.

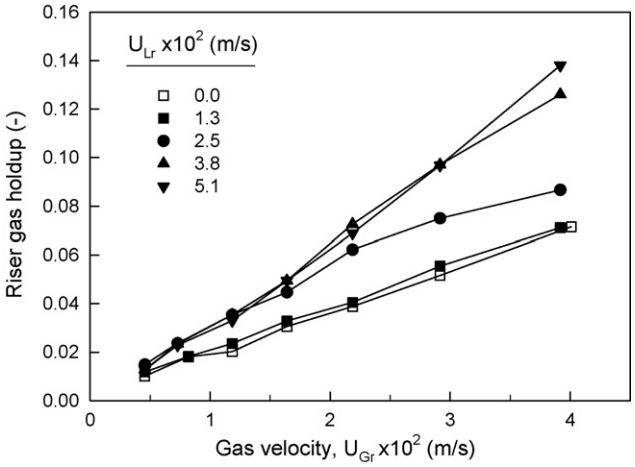

Fig. 6. Influence of superficial gas velocity (U_{Gr}) and forced circulation liquid velocity (U_{Lr}) on gas holdup in riser.

ity of 1.3×10^{-2} m/s when compared with operation in the airlift mode ($U_{Lr} = 0$ m/s, Fig. 6).

In Fig. 4, a forced circulation liquid velocity of 1.3×10^{-2} m/s was seen to substantially increase the overall gas holdup in comparison with the airlift mode of operation. A significantly lower effect of this level of liquid flow on riser gas holdup (Fig. 6) was because while increasing liquid flow increased turbulence and reduced bubble size, it also increased the superficial liquid velocity in the riser zone. An increased superficial liquid velocity reduced the residence time of the bubbles in the riser zone and counteracted the gas holdup increasing effect of increased turbulence.

Increasing liquid flow rate reduced bubble size and increased riser gas holdup only up to a liquid velocity of 3.8×10^{-2} m/s (Fig. 6). A further increase in liquid velocity to 5.1×10^{-2} m/s had barely any effect on the riser gas holdup. As explained earlier, the elevated superficial liquid velocity was counteracting the gas holdup enhancing effect of increased turbulence.

The downcomer gas holdup varied with the gas and liquid velocities, as shown in Fig. 7. During operation in the air-

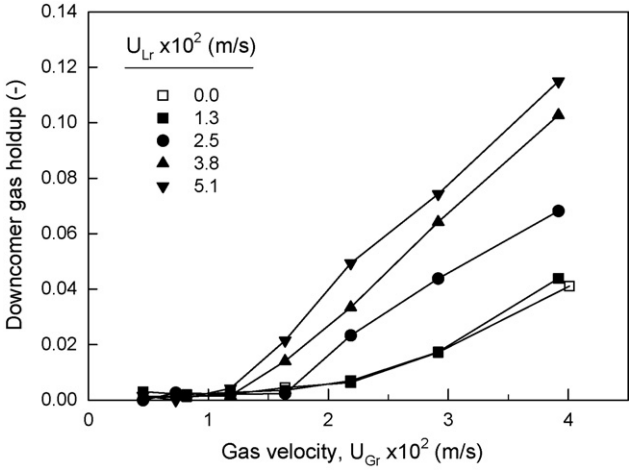

Fig. 7. Downcomer gas holdup (ε_d) vs. superficial gas velocity (U_{Gr}) for various values of superficial liquid velocity due to forced circulation (U_{Lr}).

lift mode and at the lowest value of the liquid injection rate ($U_{Lr} = 1.3 \times 10^{-2}$ m/s), barely any gas bubbles were dragged into the downcomer zone because of a low value of the downcomer liquid velocity. Consequently, there was barely any gas holdup in the downcomer under these conditions (Fig. 7). A significant number of bubbles began to be dragged into the downcomer once the velocity of gas in the riser exceeded $\sim 2 \times 10^{-2}$ m/s (Fig. 7). The value of the gas flow rate at which the downcomer attained a significant gas holdup, reduced with increasing rate of forced liquid flow (Fig. 7). This was because the imposed liquid flow was directly adding to the superficial liquid velocity in the downcomer, to enhance dragging of the gas bubbles into the downcomer zone. Although an increase of forced flow liquid velocity from 3.8×10^{-2} m/s to 5.1×10^{-2} m/s had not increased the riser gas holdup (Fig. 6), it did significantly enhance the downcomer gas holdup (Fig. 7) as more bubbles were dragged in the downcomer because of a high flow rate of liquid.

Liquid circulation in an airlift loop that does not involve forced flow of liquid, is driven exclusively by the difference in gas holdup values between the riser and downcomer zones. As shown in Fig. 8, for the forced circulation mode of operation also, a significant difference between riser and downcomer gas holdup values always existed even at quite high values of forced circulation rate. Thus, airlift action always contributed to liquid circulation in the riser–downcomer loop. Nonetheless, the difference in gas holdup, i.e. $(\varepsilon_r - \varepsilon_d)$, was lower at high gas flow rates when a high level of forced circulation ($U_{Lr} = 5.1 \times 10^{-2}$ m/s) was used in comparison with the case of the lower forced liquid flow velocity value of 3.8×10^{-2} m/s (Fig. 8). This was because at high rates of forced circulation the liquid dragged more bubbles in the downcomer, increased the downcomer gas holdup and therefore reduced the holdup difference $(\varepsilon_r - \varepsilon_d)$.

For all combinations of gas and liquid flow rates, the overall gas holdup in the reactor correlated with the superficial air velocity (U_{Gr}) in the riser zone and the total specific power input

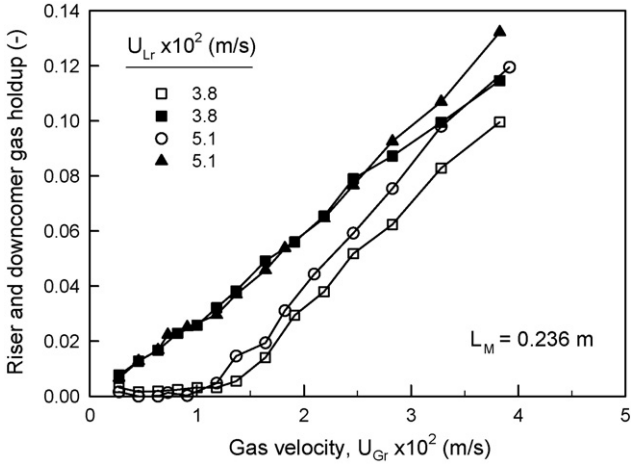

Fig. 8. Riser gas holdup (solid symbols) and downcomer gas holdup (hollow symbol) vs. superficial gas velocity (U_{Gr}) at two values of forced circulation superficial liquid velocity (U_{Lr}).

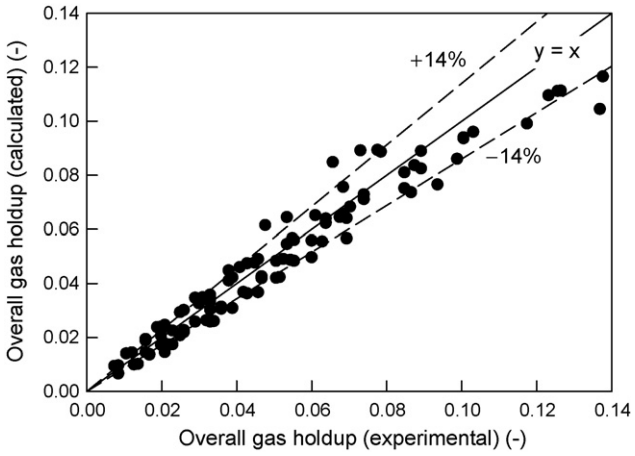

Fig. 9. Calculated (Eq. (3)) vs. measured overall gas holdup.

(e_T), as follows:

$$\varepsilon = 0.603 U_{Gr}^{0.912} e_T^{0.018} \quad (3)$$

Gas holdup values estimated with Eq. (3) agreed with the experimentally measured data within ±14% average deviation (Fig. 9).

Fig. 10 compares the gas holdup data obtained in the airlift mode of operation ($U_{Lr} = 0$ m/s) and forced circulation operation with the following correlation that has been reported [6,12] for bubble columns:

$$\varepsilon = 2.47 U_G^{0.97} \quad (4)$$

Eq. (4) applies to air–water system in bubble flow regime ($U_G \leq 0.04$ m/s) and has been shown to correlate well a large amount of published data [6,12]. For any value of the superficial gas velocity in Eq. (4), the corresponding specific power input was calculated with the following well-established equation for bubble columns [6]:

$$e_T = \rho_L g U_G \quad (5)$$

For comparable ranges of specific power inputs, the airlift mode of operation of the loop reactor produced lower values of gas

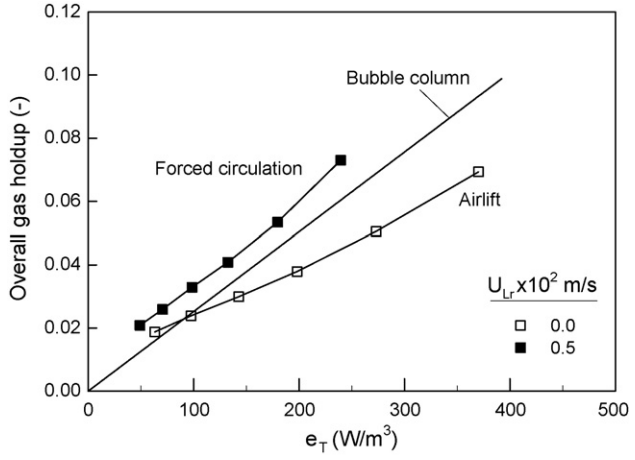

Fig. 10. Comparison of overall gas holdup in airlift and forced circulation modes of operation, with bubble columns (Eq. (4)).

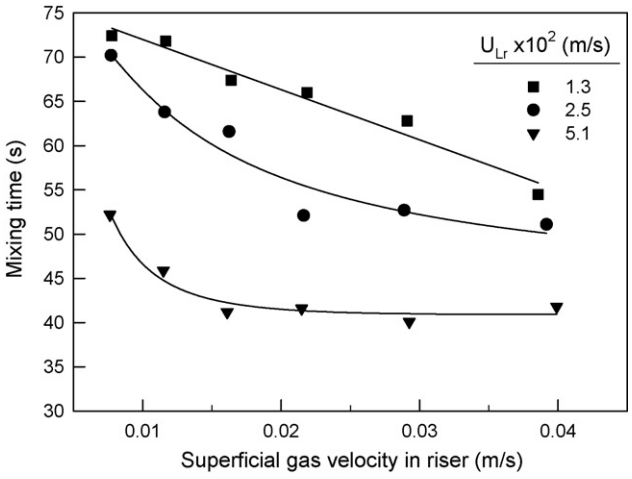

Fig. 11. Mixing time vs. superficial gas velocity in riser, for different values of forced circulation superficial liquid velocity (U_{Lr}).

holdup than predicted by Eq. (4). This is consistent with the well known behavior of airlift reactors in which the superimposed liquid flow in the riser zone increases the rise velocity of gas bubbles, therefore, lowering gas holdup compared with bubble columns operated without a net flow of liquid. In the forced circulation mode, the loop reactor produced distinctly and consistently higher values of gas holdup than predicted (Eq. (4)) for bubble columns. This was a consequence of the small size of gas bubbles in the loop reactor because the bubbles were broken by turbulence caused by forced flow of the liquid phase.

3.3. Mixing time

Dependence of mixing time on gas and liquid flow rates is shown in Fig. 10. Mixing time decreased with increasing values of both gas and liquid flow rates. Mixing time versus aeration rate curves in bubble column and airlift reactors can be characteristically divided into two regions [13]. Typically, at low aeration rates mixing time is highly sensitive to aeration rate, but at higher values of aeration rate mixing time is no longer influenced by aeration rate [13,14]. This characteristic behavior was clearly seen for the forced circulation loop reactor at the two high values of forced liquid flow rates that were tested (Fig. 11). At low aeration rates, i.e. $U_{Gr} \leq 0.015$ m/s, the sensitivity of mixing time to aeration velocity increased with increased value of the forced liquid circulation rate (Fig. 11).

4. Conclusions

Gas holdup and mixing in a forced circulation loop reactor were characterized for various combinations of gas and liquid flow rates. Presence of forced liquid flow enabled the bubble flow regimen to be maintained under operating conditions that would have otherwise produced heterogeneous churn-turbulent flow. Use of forced flow of liquid provided a means of significantly increasing the value of gas holdup compared with operation as an airlift reactor without the forced flow. Both gas and liquid flow rates contributed to promoting mixing in the reactor. Potentially, forced liquid flow circulating internal loop reactors as used here can produce substantially higher values of gas holdup and gas–liquid interfacial area when compared with equivalent airlift reactors operated at comparable levels of power input.

References

[1] A. Fadavi, Y. Chisti, Gas–liquid mass transfer in a novel forced circulation loop reactor, Chem. Eng. J. 112 (2005) 73–80.
[2] H. Blenke, Loop reactors, Adv. Biochem. Eng. 13 (1979) 120–214.
[3] U. Wachsmann, N. Räbiger, A. Vogelpohl, The Compact reactor—a newly developed loop reactor with a high mass transfer performance, Ger. Chem. Eng. 7 (1984) 39–44.
[4] U. Wachsmann, N. Räbiger, A. Vogelpohl, Effect geometry on hydrodynamics and mass transfer in compact reactor, Ger. Chem. Eng. 8 (1985) 411–418.
[5] A. Fadavi, Circulation reactor. Patent application SK4135U, Industrial Property Office of Slovak Republic, 2004.
[6] M.Y. Chisti, Airlift Bioreactors, Elsevier, London, 1989.
[7] K. Bohner, H. Blenke, Gsgehalt und flüssigkeitsumwälzung im Schlaufenreaktor, Verfahrenstechnik 6 (1972) 50–57.
[8] P. Havelka, V. Linek, J. Sinkule, J. Zahradnik, M. Fialova, Effect of the ejector configuration on the gas suction rate and gas hold-up in ejector loop reactors, Chem. Eng. Sci. 52 (1997) 1701–1713.
[9] J.M. Coulson, J.F. Richardson, J.R. Backhurst, J.H. Harker, Chemical Engineering, vol. 1, 4th ed., Pergamon, Oxford, 1990.
[10] Y.T. Shah, G.J. Stiegel, M.M. Sharma, Backmixing in gas–liquid reactors, AIChE J. 24 (1978) 369–400.
[11] M. Gavrilescu, R.V. Roman, R.Z. Tudos, Hydrodynamics in external-loop airlift bioreactors with static mixers, Bioprocess Eng. 16 (1997) 93–99.
[12] Y. Chisti, M. Moo-Young, Gas holdup in pneumatic reactors, Chem. Eng. J. 38 (1988) 149–152.
[13] F. Wenge, Y. Chisti, M. Moo-Young, Split-cylinder airlift reactors: hydraulics and hydrodynamics of a new mode of operation, Chem. Eng. Commun. 155 (1996) 19–44.
[14] Y. Chisti, Pneumatically agitated bioreactors in industrial and environmental bioprocessing: hydrodynamics, hydraulics and transport phenomena, Appl. Mech. Rev. 51 (1998) 33–112.